Separated Double-Current Layers in a High-Guide-Field Reconnection Experiment

Kyohei KONDO, Michiaki INOMOTO, Xuehan GUO, Tomohiko USHIKI, Takumichi SUGAWARA, Takumi MIHARA, Shuji KAMIO[1)], Hiroshi TANABE and Yasushi ONO

Graduate School of Frontier Sciences, The University of Tokyo, Kashiwa 277-8561, Japan
[1)]*National Institute for Fusion Science, Toki 509-5292, Japan*

(Received 1 May 2017 / Accepted 22 June 2017)

Magnetic reconnection in the presence of a high-guide-field is utilized to heat the plasma in the merging start-up of a spherical tokamak configuration. The reconnection current layer between two spherical tokamaks was gradually compressed, and a quasi-steady current-sheet thickness was obtained. During the compression phase, the current layer split transiently into two separated layers, which provided a flattened magnetic-field-region near the X-point. This modification may affect the electron-energization mechanism in the merging start-up of a spherical tokamak in a high-guide-field.

Keywords: magnetic reconnection, spherical tokamak, plasma merging, current layer

DOI: 10.1585/pfr.12.1202033

The spherical tokamak (ST) concept [1] provides attractive features such as high toroidal beta and a high bootstrap-current fraction. However, the size of the center-solenoid coil must be reduced owing to the small space near the central axis. One center-solenoid-free start-up method is the merging formation that has been developed in the TS-3/4 [2], UTST [3], and START/MAST [4] devices. In the merging formation, two STs are inductively formed using poloidal-field coils and are then merged into one ST via magnetic reconnection [5] of the poloidal fields of the two initial STs. This rapidly converts magnetic energy to plasma kinetic/thermal energy.

In the merging start-up of an ST, a strong toroidal magnetic field, which is perpendicular to the reconnecting magnetic field, acts as a "guide field," magnetizing the plasma particles even at the reconnection X-point and changing the global/microscopic behavior of reconnection [6]. A unique feature of guide-field-assisted reconnection is that electrons are effectively accelerated along the guide field via the reconnection electric field. The maximum energy attained by the electrons is affected both by the reconnection electric field and the ratio of the toroidal (guide) magnetic field to the poloidal (reconnection) magnetic field [7, 8]. In this study, we investigate the detailed structure of the reconnection magnetic field around the X-point of a high-guide-field reconnection event in the UTST merging experiment.

Figure 1 shows the magnetic flux surfaces observed at an early phase of an ST merging experiment via a 2D pickup-coil array whose locations are indicated by the small "x"s in the figure. The time evolutions of the reconnected magnetic flux and of the reconnection electric field are shown in Figs. 2 (a) and (b). The plasma merging is completed within ~60 μs because the poloidal magnetic flux contained in each of the initial STs is limited. The reconnection electric field reached ~100 V/m in the middle of the merging period. This high electric field accelerates the electrons in the region wherein the poloidal magnetic field is much weaker than that of the toroidal magnetic field.

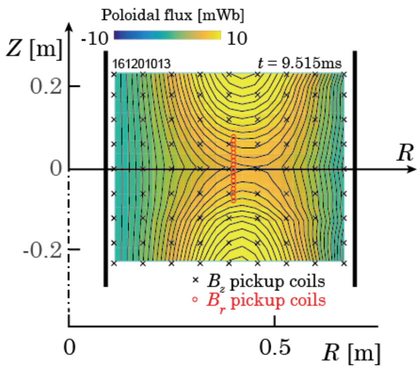

Fig. 1 Magnetic flux surfaces (spacing: 0.5 mWb) observed in an early phase of the UTST merging experiment.

The detailed structure of the reconnection magnetic field B_r was measured via a 1D pickup-coil array at intervals of 1 cm, as shown by the small red circles in Fig. 1. The time evolution of the current-layer thickness obtained using the fitting of the Harris-type function [9] to the B_r data is shown in Fig. 2 (c). A wider current layer was formed in the early phase when the two initial STs re-

author's e-mail: kondo@ts.k.u-tokyo.ac.jp

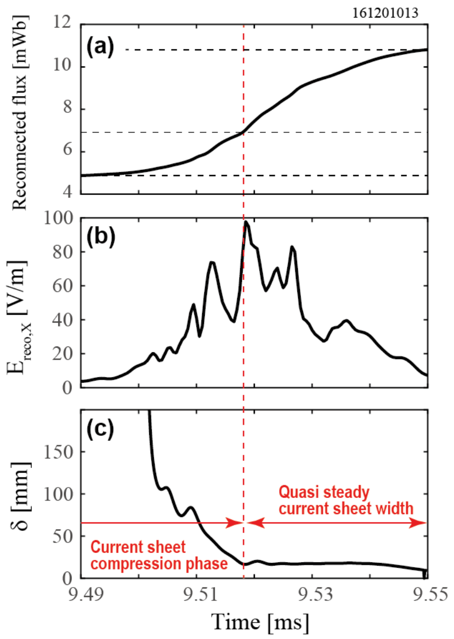

Fig. 2 Time evolution of (a) reconnected magnetic flux, (b) reconnection electric field, and (c) current layer thickness.

mained separated. The current layer was then gradually compressed, and a quasi-steady current layer of thickness $\delta \sim 14$ - 18 mm was observed in the later phase wherein $t > 9.52$ ms. Because 30% of the total flux was reconnected during the current-sheet-compression phase, effective energization in this dynamic period is required to achieve a high heating efficiency.

Figure 3 (a) shows the profile of the reconnection field B_r across the current layer as measured at $t = 9.514$ ms during the compression phase. The blue curve shows a Harris-type function with five free parameters (a, b, c, d, and Z_0),

$$a \tanh\left(\frac{Z - Z_0}{d}\right) + bZ + c, \qquad (1)$$

fitted to the data points. It is clear that the field profile is not well described by the Harris-type function. Note that the difference between the experimental data and the fitted curve is much larger than the typical measurement error $\sigma \sim 0.2$ mT at each coil location. This difference arises from a poor choice of the fitting function. We obtained a much better approximation when we employed a modified Harris-type function containing two tanh terms with eight free parameters (a_1, a_2, b, c, d_1, d_2, Z_{01}, and Z_{02}):

$$a_1 \tanh\left(\frac{Z - Z_{01}}{d_1}\right) + a_2 \tanh\left(\frac{Z - Z_{02}}{d_2}\right) + bZ + c. \qquad (2)$$

This function is shown by the red curve in Fig. 3 (a). The current-density profile shown in Fig. 3 (b) reveals the expected double-current-layer structure separated in the Z direction. In later phases, after the current sheet has been sufficiently compressed, the magnetic field is well described by a simple Harris-type function with one tanh term, as shown in Figs. 3 (c) and (d).

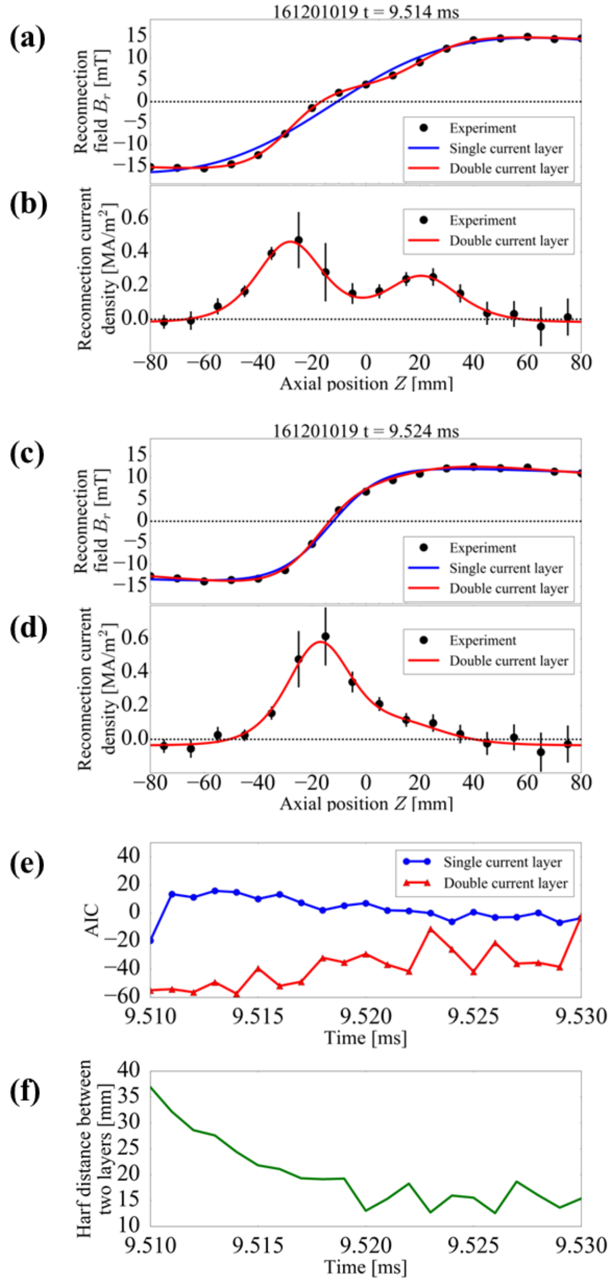

Fig. 3 Measured $B_r(Z)$ profiles (closed circles) and fitted curves corresponding to a single Harris-type function (blue) and a double Harris-type function (red) at $t = 9.514$ ms (a) and 9.524 ms (c). Panels (b) and (d) show the current-density profiles calculated from the measured data (closed circles) with 3δ error bars and Harris-type functions (red) that assume the radial differential of the reconnected field B_z is negligibly small. Panel (e) shows the time evolution of the quantity AIC for fittings using single/double current-layer models. Panel (f) shows the half-distance between the two current layers obtained from a double Harris-type function.

Figure 3 (e) shows the time evolution of Akaike's Information Criterion (AIC) [10] for fittings using both single- and double-layer Harris-type functions. Though the double-layer model includes more free parameters than the single-layer model, it provides a more accurate representation of the experimental results, particularly in the early reconnection phase wherein the AIC for the double-layer fitting is much smaller than that for the single-layer fitting. During the sheet-compression phase, the reconnection field structure was modified, and a transient double-current-layer configuration was formed. Figure 3 (f) shows the evolution of the half-distance between the two current layers obtained from the fitted double-Harris-type function. The "sheet-compression" process can be adequately interpreted as two current layers approaching each other. The modified field profile changes the electron-energization mechanism because (a) effective electron acceleration occurs in a wider area around the X-point region and (b) electron heating is located in the outer regions where the current density peaks. Further experimental study using electron-temperature/velocity-distribution measurements is required to verify the effect of the modified magnetic field structure in high-guide-field reconnection.

This work was supported by JSPS A3 Foresight Program "Innovative Tokamak Plasma Startup and Current Drive in Spherical Torus," Grant-in-Aid for Scientific Research (KAKENHI) 26287143, 15H05750, 15K14279, 16K14525, and the NIFS Collaboration Research Program NIFS15KBAR012.

[1] Y.-K.M. Peng, Phys. Plasmas **7**, 1681 (2000).
[2] Y. Ono *et al.*, Plasma Phys. Control. Fusion **54**, 124039 (2012).
[3] M. Inomoto *et al.*, Nucl. Fusion **55**, 033013 (2015).
[4] H. Tanabe *et al.*, Nucl. Fusion **57**, 056037 (2017).
[5] M. Yamada, R. Kulsrud and H. Ji, Rev. Mod. Phys. **82**, 603 (2010).
[6] J.F. Drake *et al.*, Phys. Rev. Lett. **94**, 095001 (2005).
[7] G. Lapenta *et al.*, Phys. Plasmas **17**, 082106 (2010).
[8] T. Ushiki *et al.*, Plasma Fusion Res. **11**, 2402100 (2016).
[9] M. Yamada *et al.*, Phys. Plasmas **7**, 1781 (2000).
[10] H. Akaike, IEEE Trans. Autom. Control, **19**, 716 (1974).